Available online at www.sciencedirect.com
ScienceDirect
Journal of Computational and Applied Mathematics 215 (2008) 378–389
JOURNAL OF COMPUTATIONAL AND APPLIED MATHEMATICS
www.elsevier.com/locate/cam

Second order blended multidimensional upwind residual distribution scheme for steady and unsteady computations☆

Jiří Dobeš[a, b, *], Herman Deconinck[a]

[a] *Von Karman Institute, Waterloosesteenweg 72, B-1640 Rhode-St-Genese, Belgium*
[b] *Department of Technical Mathematics, Faculty of Mechanical Engineering, Czech Technical University, Karlovo Nám. 13, CZ-121 35 Prague, Czech Republic*

Received 12 July 2005

Abstract

Multidimensional upwind residual distribution (RD) schemes have become an appealing alternative to more widespread finite volume and finite element methods (FEM) for solving compressible fluid flows. The RD approach allows to construct nonlinear second order and non-oscillatory methods at the same time. They are routinely used for steady state calculations of the complex flow problems, e.g., 3D turbulent transonic industrial-type simulations [H. Deconinck, K. Sermeus, R. Abgrall, Status of multidimensional upwind residual distribution schemes and applications in aeronautics, AAIA Paper 2000-2328, AIAA, 2000; K. Sermeus, H. Deconinck, Drag prediction validation of a multi-dimensional upwind solver, CFD-based aircraft drag prediction and reduction, VKI Lecture Series 2003-02, Von Karman Institute for Fluid Dynamics, Chausée do Waterloo 72, B-1640 Rhode Saint Genèse, Belgium, 2003].

Despite its maturity, some problems are still present for the nonlinear schemes developed up to now: namely a poor iterative convergence for the transonic problems and a decrease of accuracy in smooth parts of the flow, caused by a weak L_2 instability [M. Ricchiuto, Construction and analysis of compact residual discretizations for conservation laws on unstructured meshes. Ph.D. Thesis, Université Libre de Bruxelles, Von Karman Institute for Fluid Dynamics, 2005].

We have developed a new formulation of a blended scheme between the second order linear LDA [R. Abgrall, M. Mezine, Residual distribution scheme for steady problems, 33rd Computational Fluid Dynamics course, VKI Lecture Series 2003-05, Von Karman Institute for Fluid Dynamics, Chausée do Waterloo 72, B-1640 Rhode Saint Genèse, Belgium, 2003] scheme and the first order N scheme. The blending coefficient is based on a simple shock capturing operator and it is properly scaled such that second order accuracy is preserved. The approach is extended to unsteady flows problems using consistent formulation of the LDA scheme with the mass matrix [M. Mezine, M. Ricchiuto, R. Abgrall, H. Deconinck, Monotone and stable residual distribution schemes on prismatic space–time elements for unsteady conservation laws, 33rd Computational Fluid Dynamics Course, Von Karman Institute for Fluid Dynamics, 2003; R. Abgrall, M. Mezine, Construction of second order accurate monotone and stable residual distribution schemes for unsteady flow problems, J. Comput. Phys. 188 (2003) 16–55]. For the time integration, a three point backward scheme is selected for its accuracy and robustness and the shock capturing operator is modified appropriately, to handle moving shocks.

☆ This work was partially supported by the Research Plan MSM of the Czech Republic No. 6840770003.
* Corresponding author. Von Karman Institute, Waterloosesteenweg 72, B-1640 Rhode-St-Genese, Belgium.
E-mail address: jiri.dobes@fs.cvut.cz (J. Dobeš).

0377-0427/$ - see front matter
doi:10.1016/j.cam.2006.03.046

We present a numerical solution of several challenging test cases involving the solution of the Euler equations from the subsonic to the hypersonic regime. All the tests shows very good accuracy, robustness and convergence properties.

MSC: 65M99; 35L65; 76M10; 76M12

Keywords: Residual distribution scheme; Fluctuation splitting scheme; Steady problems; Unsteady problems; Finite volume method; Finite element method; Transonic flows; Shock capturing; Mass matrix; Implicit method

1. Introduction

The class of compact residual distribution (RD) schemes has become an appealing alternative for solving fluid flows to other approaches, as e.g., finite volume (FV) and finite element methods (FEM). RDS combine the second order of accuracy with non-oscillatory properties on a very compact stencil [8]. They are routinely used for steady state calculations of a complex flow problems, e.g., 3D turbulent transonic industrial-type simulations [10,20].

Among linear RD schemes, probably two of the best known schemes are the LDA and the N scheme. The LDA scheme is second order accurate scheme and it is successfully used for subsonic computations. It is not suitable for the transonic regimes, because of the oscillatory resolution of the shock waves. However, due to its upwinding character, it contains enough dissipation for medium transonic velocities. On the other hand, the N scheme is a first order, positive scheme. An example of a second order and non-oscillatory scheme is the nonlinear B scheme [10,3]. It employs a blending technique taking advantage of both the N and the LDA schemes. It performs very robustly with monotone shock capturing and it can be used for large scale applications [20]. Another approach was chosen for construction of the second order and positive N-modified (also called PSI or limited N) scheme [3]. Despite robustness of the nonlinear schemes, both the B and the N-modified schemes suffer from rather poor convergence to the steady state solution. For the implicit calculations approximation of the Jacobian by the first order scheme has to be taken, otherwise CFL numbers of order units have to be used.

The aim of the paper is to present another blending technique, which uses a shock capturing operator for blending the LDA and the N scheme. In the shock regions we use locally the N scheme for its monotone shock capturing, while in all the other regions we use the LDA scheme, because of its high accuracy. Advantage is, that the LDA scheme contains enough dissipation to resolve smooth flows and contacts discontinuities in a stable manner. The shock capturing operator is scaled such that in the smooth regions the N scheme introduces an error of higher order. Since our definition of the blending coefficient is smooth, the full Jacobian can be taken for the implicit method, which noticeably speeds up the convergence rate.

Unfortunately, a straightforward extension of the RD schemes for unsteady computations gives only first order accuracy, as was shown e.g. in [15,16,2]. The space and time derivatives cannot be written separately as they are coupled by a FEM type mass matrix. Since this matrix is not a M-matrix, simple inversion leads to an oscillatory scheme, even if the underlying spatial scheme was shown to be non-oscillatory. A first attempt was to use the flux corrected transport (FTC) method to construct a non-oscillatory scheme, but it was only moderately successful [15,13,14]. An another approach is the construction of the space–time scheme and to apply the RD schemes in space–time [6,7,16,2]. Unfortunately, nonlinear versions of these schemes also suffer from erratic convergence in dual (or pseudo) time for transonic computations. There is also a version of the N-limited space–time scheme for arbitrary time step [16], but taking a CFL number higher than order of decade practically prevents convergence in pseudo-time. Moreover this version uses twice more unknowns, which can bring some difficulties for solving large 3D problems.

For time dependent problems we present the version of the blended scheme, which uses the spatial LDA scheme with consistent mass matrix and as a non-oscillatory scheme the N scheme with the lumped mass matrix. Both methods employs the three point backward time integration scheme in the physical time. The resulting system of nonlinear equations is solved in dual time by mean of a explicit or implicit time integration. The shock capturing operator is modified by inclusion of the time derivative of the pressure to account for unsteady shocks. Since the formulation of both the LDA and N scheme is stable for arbitrary physical time step, we expect, that the resulting scheme Bx can be used for industrial-type of simulations with high CFL numbers.

The paper is organized as follows: in the following section we show how the shock capturing operator is constructed and we point out differences between the present and the standard definition of the B scheme. Then we present test cases for steady problems. We give the definition of the time accurate version of the schemes and show how the shock capturing operator is constructed for the unsteady problems. After presentation of numerical results we conclude.

2. RD schemes for steady problem

In this section we are interested in a steady solution u of the Euler equations in conservative form

$$u_t + \vec{\nabla} \cdot \vec{f} = 0, \tag{2.1}$$

where $\vec{f}$ is the vector of fluxes. The system is closed by the equation for perfect gas with the specific heat ratio $\gamma = 1.4$.

The solution at time level $n+1$ is computed by the relation

$$U_i^{n+1} = U_i^n - k_i \sum_{T \in i} \phi_i^{\mathrm{T}}, \tag{2.2}$$

where U_i is the solution in node i, k_i is a constant depending on the stability of the iteration procedure and ϕ_i^{T} is the contribution from the element T, sharing node i, to the node i given by the particular scheme. In the case of the LDA scheme, the nodal contribution is given by

$$\phi_i^{\mathrm{LDA}} = -K_i^+ N \phi^{\mathrm{T}}, \quad N = \left(\sum_{j \in T} K_j^+ \right)^{-1}, \quad K_i = \frac{\partial \vec{F}}{\partial U} \frac{\vec{n}_i}{d}, \tag{2.3}$$

where K_i^+ is the positive-eigenvalue part of the upwind matrix K_i, evaluated in a mean state given by linearization [9], $\vec{n}_i$ is the inward normal to the face opposite to the node i scaled by its surface and ϕ^{T} is the element residual given by $\phi^{\mathrm{T}} = \sum_{j \in T} K_j \bar{U}_j$, where $\bar{U}_j$ are nodal values evaluated according to linearization [9]. The number of spatial dimensions is d ($d = 2$ for 2D). The summation is performed over all the nodes j contained in element T. The N scheme is given by

$$\phi_i^{\mathrm{N}} = K_i^+ (\bar{U}_i - U_{\mathrm{in}}), \quad U_{\mathrm{in}} = N \left(\sum_{j \in T} K_j^- \bar{U}_j \right). \tag{2.4}$$

The original blended B scheme [10,3] constructed from the N and the LDA scheme, is given by

$$\phi_i^{\mathrm{B}} = \theta \phi_i^{\mathrm{N}} + (1-\theta) \phi_i^{\mathrm{LDA}}, \quad \theta = \frac{|\phi^{\mathrm{T}}|}{\sum_{j \in T} |\phi_j^{\mathrm{N}}|}, \tag{2.5}$$

where θ is computed for each component of the vector of unknowns U_i. The scheme is second order accurate, because it poses the residual property [1,3], i.e., if the element residual $\phi^{\mathrm{T}} = 0$ the element contribution $\phi_i^{\mathrm{B}} = 0$.

3. New formulation of blended (Bx) scheme

We first construct an element-wise shock capturing sensor given by

$$\mathrm{sc} = \left(\frac{\vec{\nabla} p \cdot \vec{v}}{\delta_{pv}} \right)^+ \approx \left(\frac{\int_T \vec{\nabla} p \, \mathrm{d}x}{\delta_{pv} |T|} \cdot \vec{v} \right)^+, \tag{3.6}$$

where $\vec{v}$ is the approximation of the velocity vector in the element, p is the static pressure and $|T|$ is the area of the element. The $\delta_{pv} \approx (p_{\max} - p_{\min}) \cdot \bar{v}$ is a global pressure variation scale multiplied by the magnitude of the mean velocity in the domain. The sensor sc is positive in a shock and compression, zero in expansion, and of order $\mathrm{sc} = \mathcal{O}(1)$ in the smooth regions. One of the important properties of the scheme is its second order of accuracy. For 2D, in Eq. (2.5) the left-hand side has to give $\mathcal{O}(h^3)$ [19], where h is a diameter of a circle with the same area as the element

(or sphere in 3D). The contribution from the N scheme gives $\mathcal{O}(h^2)$ and from the LDA scheme $\mathcal{O}(h^3)$ in 2D. Hence, the blending factor θ has to be of order $\mathcal{O}(h)$. Multiplication of the shock sensor sc by h does not lead to sufficient damping in the shock regions. If multiplied by $\sqrt{h}$, then the amount of the numerical viscosity is correct, but the scheme is only $\mathcal{O}(h^{1.5})$ accurate. The solution is to take a blending factor as

$$\theta = (\mathrm{sc} \cdot \sqrt{h})^2 = \mathrm{sc}^2 \cdot h, \tag{3.7}$$

which gives the right amount of artificial viscosity together with second order of accuracy in smooth regions. The nodal contribution of the Bx scheme is then given by (2.5) with the blending coefficient given by (3.6) and (3.7).

The blending coefficient is smooth and allows us to use the full Jacobian for the implicit calculations (even though we use its numerical approximation), which noticeably speeds up the convergence rate. For all the other nonlinear schemes in this paper a first order approximation of the Jacobian had to be taken (from the N scheme).

4. Numerical results for steady problems

First, we present numerical results for transonic flow in the so-called Ni's channel [17]. The flow is defined by the ratio of the outlet static pressure to the isentropic total pressure $p_2/p_{0\mathrm{is}}$ corresponding to $M_{2\mathrm{is}} = 0.675$. The length of the channel is three with unit width and 10% circular bump. We use unstructured grid consisting of 2762 nodes and 5281 elements, with 31 nodes along the bump, utilizing Weatherill triangulation. This mesh gives a better idea of the behavior of the scheme in the case of changing connectivity, as is usual in 3D, avoids false cancellation of the error and does not prefer any direction. The Euler backward scheme is used for the time integration with numerical approximation of the Jacobian. For the N-modified and the B scheme we had to use the Jacobian of the N scheme. We start with the CFL number of 100 and every iteration we multiply it by the factor 1.2 until it reaches 10^6.

In Fig. 1 isolines of the Mach number for the present Bx scheme are shown. One can observe a supersonic pocket on the bump. The isolines do not exhibit wiggles and they run straight into the shock, which corresponds to a not very dissipative scheme. The comparison of the Mach number distribution along the bottom wall is shown on the next figure together with a zoom to the beginning and the end of the shock. Before the shock, the Bx scheme follows the LDA scheme and creates small overshoot on the Mach number distribution. After the shock the Bx scheme behaves very similar as both the N-limited and the B schemes in terms of capturing after-shock singularity. For comparison, the solution for the cell-vertex FV method with Barth limiter [4] and Roe's Riemann solver is shown. The FV scheme is clearly more dissipative than all the nonlinear RD schemes, as can be observed on the last point before the shock and mainly in the more diffusive capture of the after-shock singularity. Convergence of the norm of the residual is also present. The new formulation gives a convergence rate very similar to the linear schemes, while all the other nonlinear schemes stall after a few orders of magnitude.

The next test examines robustness of the new scheme on a Mach 20 bow shock in front of the cylinder. The solution was computed using Bx, N and N-modified scheme on the mesh consisting of 10 531 nodes and 20 632 elements. The B scheme always gives negative pressure in the shock, even if started from a converged solution with extremely small CFL number. In Fig. 2 the isolines of Mach number are shown, the left part of the figure is the N-modified scheme, while the right one presents the Bx scheme. One can note, that the Bx scheme better captures irregularities of the solution, resulting from the interaction of the shock wave with the Weatherill type of mesh. The next part of the figure shows a cut in along the streamline to the stagnation point. Points correspond to the intersection of the cut line with the edges of the triangles. As we can expect from the design of the scheme, there are no oscillations in the vicinity of the shock, nor anywhere else in the computational domain. The solution obtained by all the schemes gives practically the same result. Convergence properties of the scheme are considerably worse than for the transonic flows, as is known also from other methods. On the other hand, one can employ a convergence fix, well known from the FV framework [11]. After a certain number of iterations n_0, when the solution is fully developed, *we don't decrease anymore the blending factor* in the subsequent iterations, i.e.

$$\theta^n = \max(\theta^n, \theta^{n-1}) \quad \text{for all } n \geqslant n_0. \tag{4.8}$$

In this case we have chosen $n_0 = 4000$. It is not clear how to apply a similar fix to the N-modified scheme. Note that this definition is opposite of the FV limiter, since $\theta = 1$ gives the non-oscillatory scheme, while in the case of FV $\theta = 0$

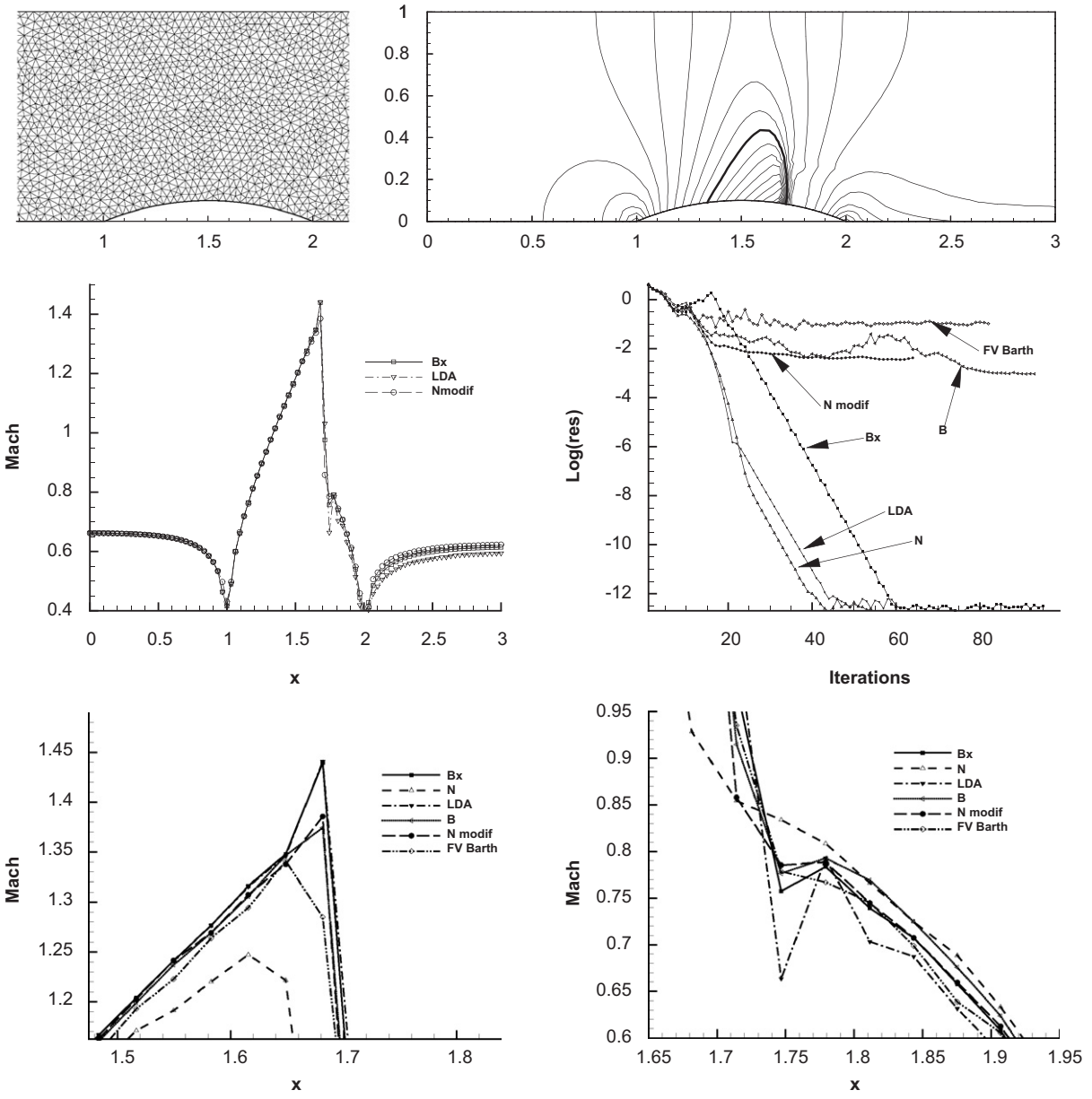

Fig. 1. Ni's channel. Top: part of the Weatherill mesh and the Mach number isolines for the Bx scheme, $\Delta M = 0.05$, the bold line is $M = 1$. Middle: the distribution of the Mach number along the bottom wall and the convergence histories for different schemes. Bottom: distribution of the Mach number along the wall, zoom before and after the shock.

reverts to the upwind scheme with constant reconstruction. The scheme recovers convergence to machine accuracy with a possibly slight price of more dissipative solution.

As the last steady case, we present a subcritical flow around the cylinder [12], with $M_\infty = 0.38$. This test examines behavior of the method in smooth flow regions. We use a much coarser mesh than in Ref. [12], because in that case all the scheme gave very similar, accurate results. Our mesh consists of approximately equilateral triangles with 80 elements along the wall and 40 rows of triangles towards the free stream boundary. This gives a position of the farfield boundary approximately 10 diameters away from the cylinder. The exact solution is perfectly symmetric both with respect to x- and y-axis. The Mach number isolines are plotted in Fig. 3 with step of $\Delta M = 0.02$. All the schemes gives reasonably good results. The LDA and present Bx gives very similar almost symmetric results, with a small deviation behind the cylinder

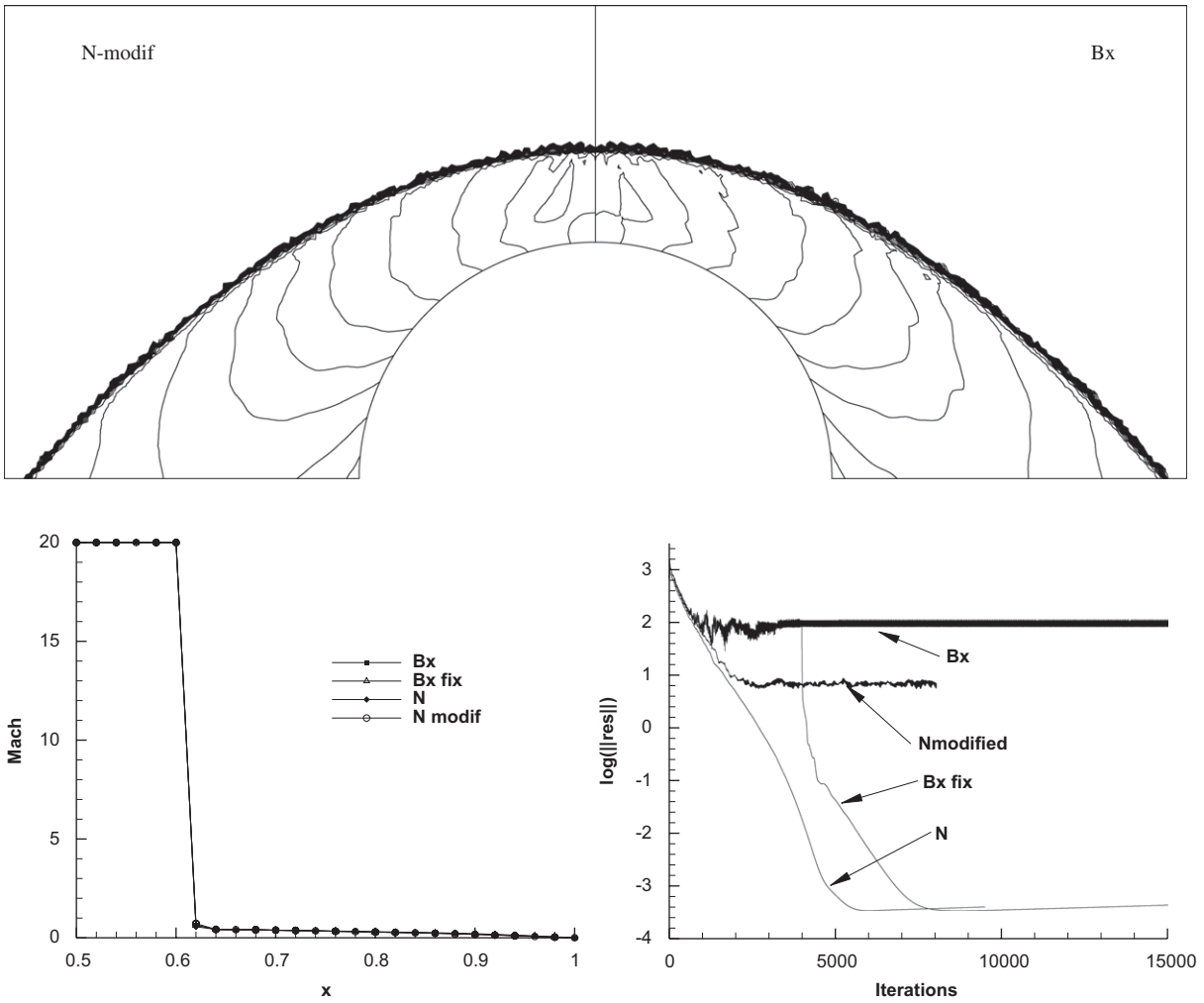

Fig. 2. Mach 20 bow shock. Top: isolines of the Mach number, the N-modified scheme is on the left, the Bx scheme on the right. Bottom: cut along the stagnation line and convergence history.

on the axis of symmetry. The standard formulation of the B scheme gives larger error behind the cylinder, however it still converges to the horizontally symmetric solution. The N-modified scheme did not converge well and wake-like structure appear behind the cylinder. However, unlike the other results in [18], no separation zone develops there. The results suggest that the Bx scheme contains very little unwanted artificial dissipation and it can capture smooth flow regions very well.

5. Blended (Bx) scheme for unsteady problems

As a basis for the blended approach for unsteady problems we use the spatial LDA scheme with the consistent mass matrix given by

$$\phi_i^{\mathrm{STLDA_m}} = \Delta t \frac{|T|}{d+1}\left(-K_i^+ N + \frac{2}{d+2} - \frac{1}{d+1}\right)\frac{\partial U_i}{\partial t} + \Delta t \frac{|T|}{d+1}\sum_{\substack{j\in T\\ j\neq i}}\left[\left(-K_j^+ N + \frac{1}{d+2} - \frac{1}{d+1}\right)\frac{\partial U_j}{\partial t}\right] - \left[\Delta t K_i^+ N \sum_{j\in T} K_j \bar{U}_j\right]^{\alpha}. \tag{5.9}$$

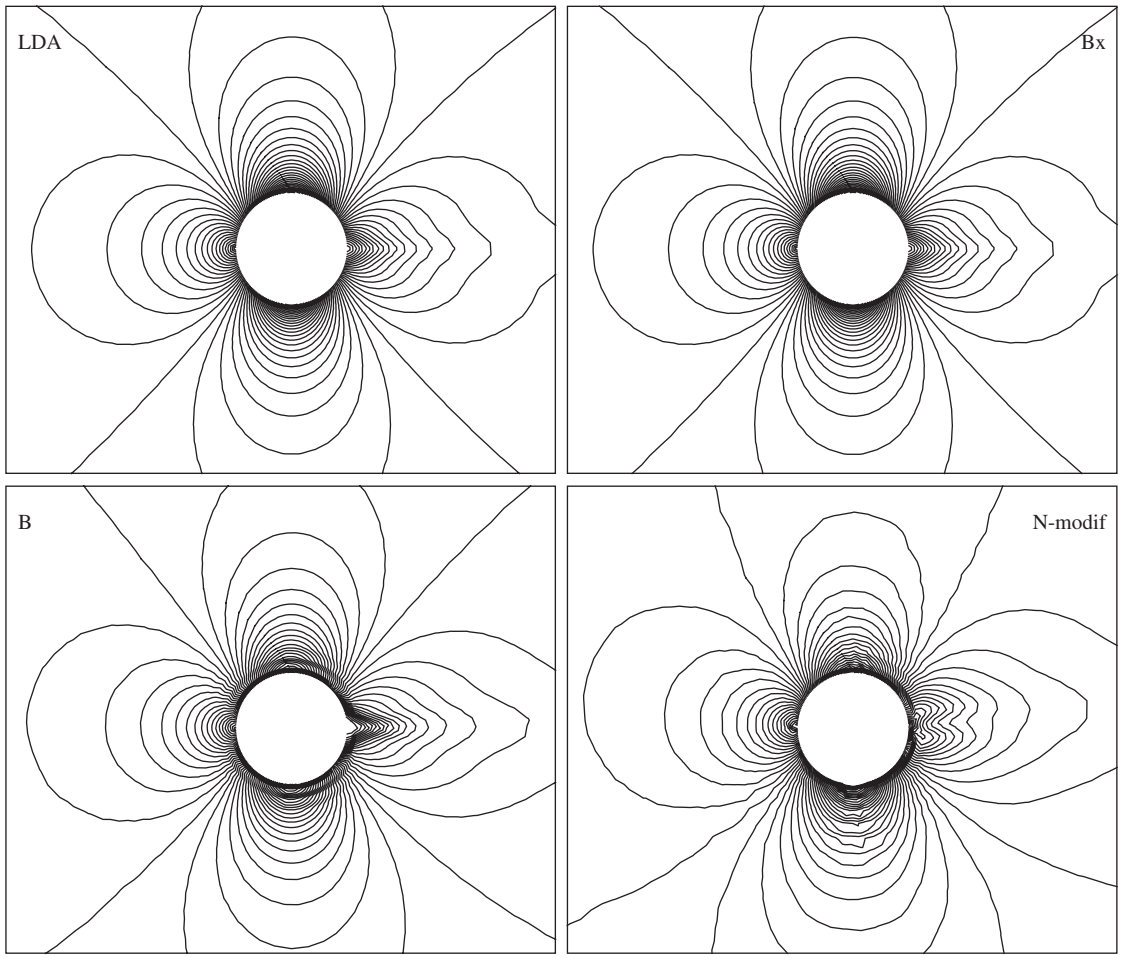

Fig. 3. Subcritical flow past the cylinder. Mach number isolines, $\Delta M = 0.02$.

In Eq. (2.2) index n has to be replaced by the pseudo-time index τ and the steady solution in pseudo time is obtained for the solution in physical time at level $n+1$ by the scheme (2.2). For the detailed derivation see e.g. [16] but there a trapezium time integration rule is used ($\alpha = n/2 + (n+1)/2$). We have chosen three points backward time integration for its superior stability. A space residual is then evaluated at time $\alpha = n+1$ and the time derivatives are discretized as

$$\frac{\partial U_i}{\partial t} = \frac{\frac{3}{2}U_i^{n+1} - 2U_i^n + \frac{1}{2}U_i^{n-1}}{\Delta t}. \tag{5.10}$$

We choose the N scheme with the lumped mass matrix and the three point backward time integration as the non-oscillatory scheme. It is given by

$$\phi_i^{\mathrm{STN_l}} = \frac{|T|}{d+1}\left(\frac{3}{2}U_i^{n+1} - 2U_i^n + \frac{1}{2}U_i^{n-1}\right) + \Delta t\, K_i^+(\bar{U}_i - U_{\mathrm{in}}). \tag{5.11}$$

The blending coefficient is modified to take into account the unsteady nature of the flow.

The change in the pressure due to the traveling pressure wave can be locally approximated as a change due to pure convection of the pressure wave and the change due to its expansion or compression. Pure convection obeys

the equation

$$\frac{\partial p}{\partial t} + \vec{v}_c \cdot \vec{\nabla} p = 0, \tag{5.12}$$

where $\vec{v}_c$ is the speed of the wave. This effect is dominant e.g., in the convection of an inviscid vortex. Pure expansions or compressions happen with respect to the frame of reference moving with velocity $\vec{v}_c$. Furthermore $\vec{v}_\mathrm{r} = \vec{v} - \vec{v}_c$, where $\vec{v}$ is the velocity of the flow and $\vec{v}_\mathrm{r}$ is relative velocity with respect to the frame of reference. The shock sensor has to be constructed *using the relative velocity*, i.e.

$$\begin{aligned} \mathrm{sc} = \frac{1}{\delta_{pv}} (\vec{\nabla} p \cdot \vec{v}_\mathrm{r})^+ &= \frac{1}{\delta_{pv}} \left(\vec{\nabla} p \cdot \vec{v}_\mathrm{r} + \underbrace{\frac{\partial p}{\partial t} + \vec{v}_c \cdot \vec{\nabla} p}_{=0} \right)^+ \\ &= \frac{1}{\delta_{pv}} \left(\frac{\partial p}{\partial t} + \vec{\nabla} p \cdot (\vec{v}_\mathrm{r} + \vec{v}_c) \right)^+ = \frac{1}{\delta_{pv}} \left(\frac{\partial p}{\partial t} + \vec{\nabla} p \cdot v \right)^+ . \end{aligned} \tag{5.13}$$

If the shock sensor is positive, the flow experiences compression, while if the argument of the shock sensor is negative, the flow is expanding with respect to the relative frame of reference. The operator is scaled in the same manner as for steady problems to define the blending coefficient, which retains the second order of accuracy of the LDA scheme together with non-oscillatory behavior.

Due to the unconditional stability of the underlying N and the LDA schemes with the three points backward time integration formula, the resulting unsteady Bx scheme is expected to be robust for high CFL number simulations.

6. Numerical results for unsteady problems

We have chosen a smooth convection of a vortex as the first unsteady test case. The problem is solved on the square domain $[-0.5, 0.5] \times [-0.5, 0.5]$ filled with Weatherill triangulation with 41 points along each side. The flow velocity is given by the mean stream velocity $\vec{v}_m = (6, 0)$ and the circumferential perturbation

$$(v_x, v_y)_\theta = (-y, x)\omega, \quad \omega = 15(\cos 4\pi r + 1), \quad r = \sqrt{x^2 + y^2} \tag{6.14}$$

for $r < 0.25$, $(v_x, v_y)_\theta = \vec{0}$ elsewhere. Density is chosen constant $\rho = 1.4$ and the pressure from the balance in the radial direction $p = p_m + \Delta p$, where,

$$\Delta p = \frac{15^2 \rho}{(4\pi)^2} \left(2\cos(4\pi r) + 8\pi r \sin(4\pi r) + \frac{\cos(8\pi r)}{8} + \frac{4\pi r \sin(8\pi r)}{4} + 12\pi^2 r^2 \right) + C. \tag{6.15}$$

The constant C is such that $p|_{r=0.25} = p_m = 100$. This setup gives maximal Mach number in the domain $M \doteq 0.8$. The free stream values are prescribed on the boundaries $y = \pm 0.5$ and periodic boundaries are used for $x = \pm 0.5$. The simulation stops after one period, i.e., $t_{\max} = \frac{1}{6}$.

In Fig. 4 the isolines of the pressure for the different schemes are shown. The computation was performed with $\mathrm{CFL}_{\mathrm{ST}} = 1$. Distribution of the pressure in the core of the vortex shows, that the Bx scheme performs essentially as the LDA scheme for the smooth regions. The performance of the N-limited scheme is noticeably worse. We have performed the same test with several other schemes. The minimal pressure in the vortex core are given in Table 1. The FV method is cell centered with the three points backward time integration scheme formulated in dual time and with, or without Barth's limiter. Note, that the FV scheme performs worse even in the case with no limiter and it uses approximately twice more unknowns than the RD scheme.

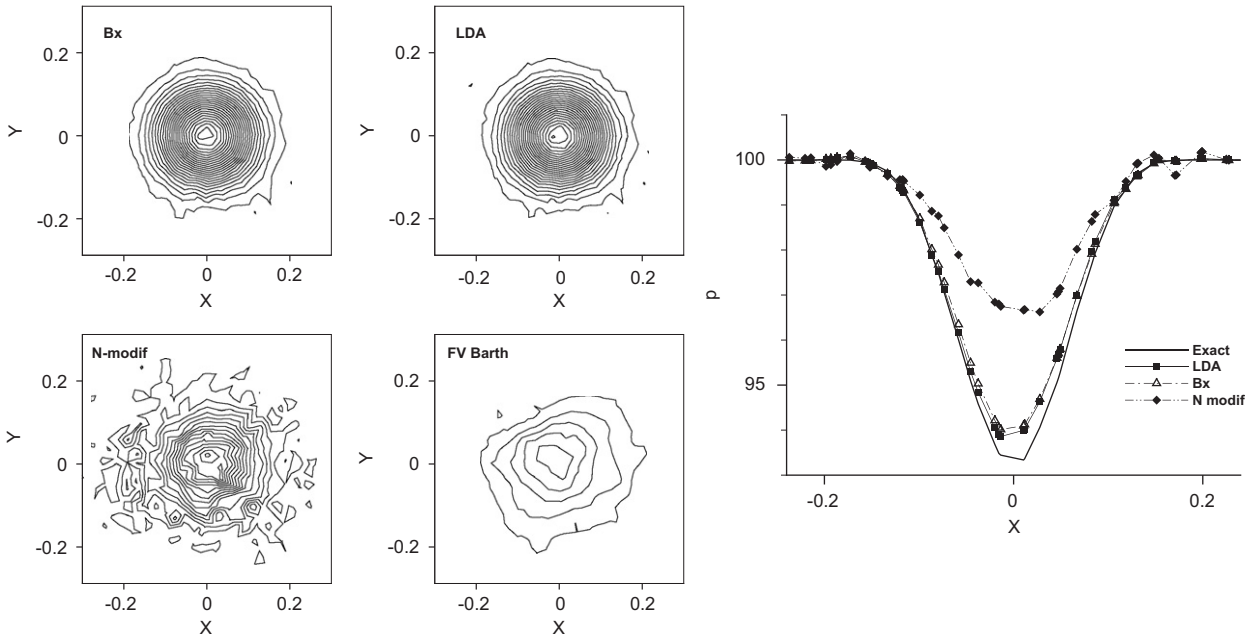

Fig. 4. Advection of the vortex, $t = \frac{1}{6}$. Isolines of the pressure for different schemes. Distribution of the pressure in the core of the vortex for different schemes.

Table 1
The maximal and the minimal pressure in the vortex core for the vortex advection problem, $t = \frac{1}{6}$

Scheme	Bx	LDA	N-limited	LDA [5]	FV nolim	FV Barth	Exact
$p_{\max}$	100.11	100.12	100.42	100.12	100.04	100.11	100
$p_{\min}$	94.00	93.84	96.27	93.88	94.35	98.76	93.213

FV is the cell centered finite volume scheme with the linear reconstruction and with or without Barth's [4] limiter and the three point backward scheme formulated in dual time.

As a test to examine the scheme on a complex flow features, we present results for a 2D Riemann problem [16]. The problem is symmetric along $y = x$ with the initial conditions given by

$$(\rho, v_x, v_y, p) = \begin{cases} (1.5, 0, 0, 1.5) & y < 0.8, \quad y > x \\ (0.1379928, 1.2060454, 1.2060454, 0.0290323) & x > 0.8, \quad y > x \\ (0.5322581, 1.2060454, 0, 0.3) & y > x \ \text{ elsewhere.} \end{cases} \tag{6.16}$$

The simulation stops at $t_{\max} = 0.8$.

In Fig. 5 comparison of the Bx scheme with the N-modified is presented on meshes with spatial resolution $\frac{1}{200}$ and $\frac{1}{400}$. Both the computations with the Bx scheme show much higher resolution. It can be observed on pronounced Kelvin–Helmholtz instabilities along the slip lines, where the Bx scheme gives a richer structure, which is seen from the growth of the rollers along the instability. The N-modified scheme captures the instabilities well, however it clearly gives lower resolution. To show that the scheme captures the discontinuities without spurions oscillations we make a cut along the diagonal for the mesh $\frac{1}{400}$, see Fig. 5. The solution obtained by the Bx scheme shows non-oscillatory capturing of the smooth regions as well as discontinuities. On the other hand, there are undamped high frequency modes on the solution given by the N-modified scheme, which causes oscillations in the smooth regions of the solution.

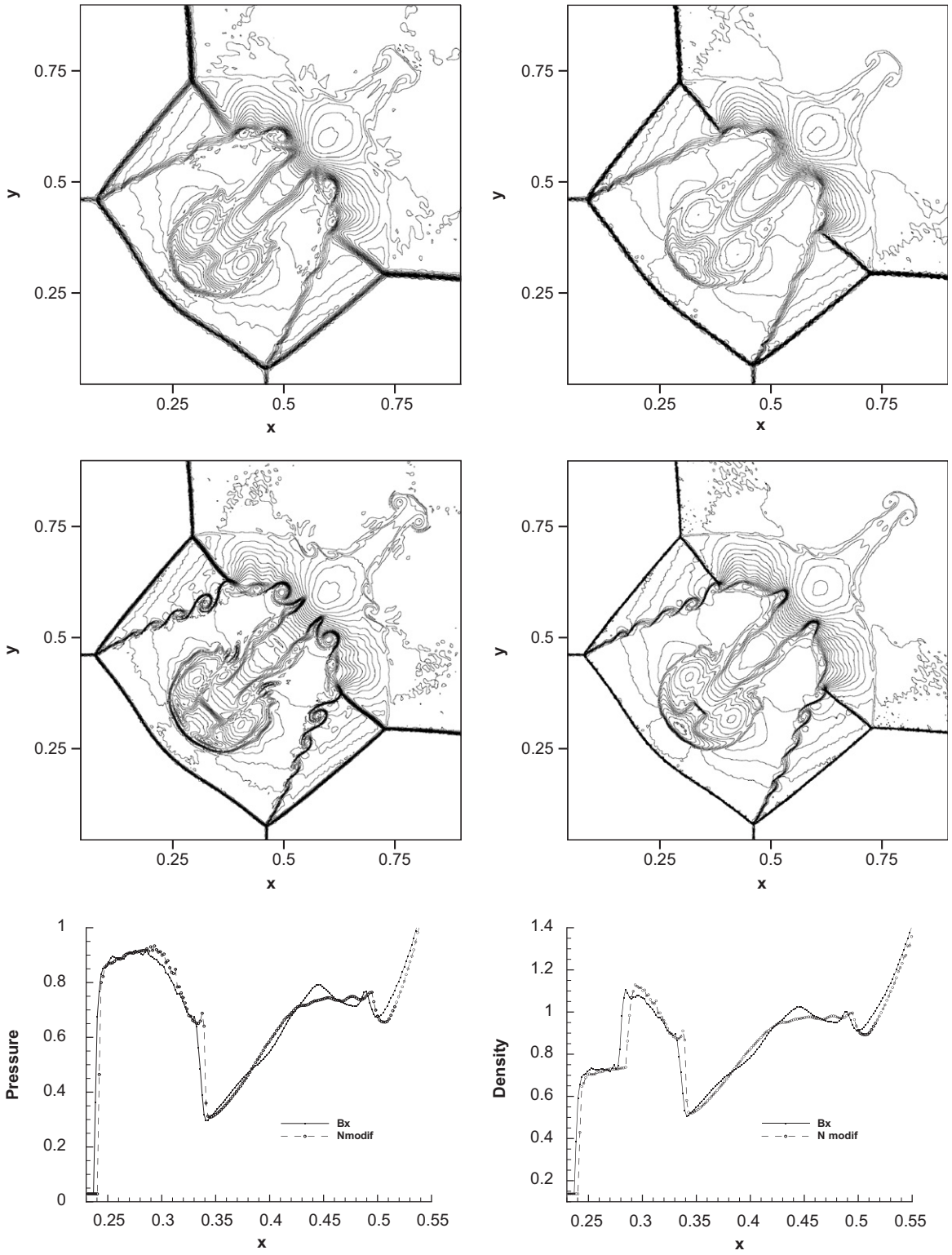

Fig. 5. 2D Riemann problem, density contours ($\Delta\rho = 0.05$) at $t = 0.8$. Left figures show the solution obtained by the Bx scheme, while right figures show the results of the N-modified scheme. Top row: spatial resolution $\frac{1}{200}$, middle row $\frac{1}{400}$. Bottom: solution along the diagonal for the mesh $\frac{1}{400}$ for the pressure and the density is shown in the last row.

7. Conclusions

A new formulation for nonlinear blending of residual distribution (RD) schemes was developed. As a basis, the LDA and the N schemes were chosen to assembly the new Bx scheme, both schemes for their robustness, the LDA for its accuracy and the N for its non-oscillatory shock capturing. Then, the blending coefficient was constructed on a basis of the shock capturing operator, which is $\mathcal{O}(1)$ in the smooth regions. The shock capturing term is then scaled such that the blending coefficient is of order $\theta = \mathcal{O}(h)$ in the smooth regions. Since the LDA scheme is second order accurate and the $\mathcal{O}(h)$ error coming from the N scheme is multiplied by θ, it gives second order accuracy of the resulting scheme in smooth regions. The blending coefficient is constructed such that it does not introduce any additional dissipation in a shear layer, namely in the boundary layer. This is an advantage for later extension of the scheme to viscous computations, since the inherent stability of the LDA scheme in the boundary layer is usually sufficient.

Unlike other formulations of nonlinear RD schemes, the Bx scheme has very good iterative convergence properties, since the blending coefficient is smooth and well defined. Moreover, a well-known convergence fix from the finite volume (FV) framework can be applied to improve iterative convergence for the computations for very high Mach numbers, both for the steady and the unsteady case. Because of the smooth behavior of the scheme, the consistent Jacobian for the implicit calculations can be used with advantage. In this case, recovery of the quadratic convergence for the Newton method can be expected.

The Bx scheme was tested on several challenging cases, including subcritical flow around a circular cylinder, Mach 20 bow shock and transonic flow in the 10% circular bump channel. In all the cases the scheme has performed very well, in the smooth regions it reverts to the linear second order LDA scheme and in the regions of strong shocks it does not exhibit oscillations.

For the unsteady case, the Bx scheme is constructed on top of the LDA scheme with a consistent mass matrix and the N scheme with lumped mass matrix. Three point backward time discretization in dual time is used. The blending coefficient was modified by inclusion of the convection equation for the pressure, which turns into a contribution from the pressure time derivatives.

The convection of the vortex and a 2D Riemann problem were selected for unsteady tests. In the case of the vortex convection the Bx scheme behaves essentially like the LDA scheme, while for the Riemann problem it features the monotone shock capturing and the high accuracy off the shock region, over-performing the N-modified scheme. The Bx scheme is also much cheaper than the N-limited scheme, since no additional eigen-decomposition is needed for limiting and it features superior convergence in dual-time.

The results obtained with the Bx scheme are encouraging and justify further investigation of the scheme for 3D steady and unsteady transonic industrial-type flows.

Acknowledgments

Mario Ricchiuto has pointed out the problem with the convergence of nonlinear schemes for transonic flows and a need for a smooth blended scheme. Mario Ricchiuto is also acknowledged for the review of this article and passing me his solution of two-dimensional Riemann problem with N-modified scheme on the mesh $h = \frac{1}{400}$.

References

[1] R. Abgrall, Toward the ultimate conservative scheme: following the quest, J. Comput. Phys. 167 (2) (2001) 277–315.
[2] R. Abgrall, M. Mezine, Construction of second order accurate monotone and stable residual distribution schemes for unsteady flow problems, J. Comput. Phys. 188 (2003) 16–55.
[3] R. Abgrall, M. Mezine, Residual distribution scheme for steady problems, 33rd Computational Fluid Dynamics Course, VKI Lecture Series 2003-05, Von Karman Institute for Fluid Dynamics, Chausée do Waterloo 72, B-1640 Rhode Saint Genèse, Belgium, 2003.
[4] T.J. Barth, D.C. Jesperson, The design and application of upwind schemes on unstructured meshes, AIAA Paper 89-0366, AIAA, January 1989.
[5] D. Caraeni, M. Caraeni, L. Fuchs, A parallel multidimensional upwind algorithm for LES, AIAA Paper 2001-2547, AIAA, Anaheim, 2001, 15th AIAA Computational Fluid Dynamics Conference.
[6] A. Csík, H. Deconinck, Space–time residual distribution schemes for hyperbolic conservation laws on unstructured linear finite elements, Internat. J. Numer. Methods in Fluids 40 (2002) 573–581.
[7] Á. Csík, M. Ricchiuto, H. Deconinck, Space–time residual distribution schemes for hyperbolic conservation laws over linear and bilinear elements, 33rd Computational Fluid Dynamics Course, Von Karman Institute for Fluid Dynamics, 2003.

[8] H. Deconinck, Novel methods for convection dominated problems, 33rd Computational Fluid Dynamics Course, VKI Lecture Series 2003-05, Von Karman Institute for Fluid Dynamics, Chausée do Waterloo 72, B-1640 Rhode Saint Genése, Belgium, 2003.
[9] H. Deconinck, P.L. Roe, R. Struijs, A multidimensional generalization of Roe's flux difference splitter for the Euler equations, Comput. Fluids 22 (1993) 215–222.
[10] H. Deconinck, K. Sermeus, R. Abgrall, Status of multidimensional upwind residual distribution schemes and applications in aeronautics, AAIA Paper 2000-2328, AIAA, 2000.
[11] M. Delanaye, Polynomial reconstruction finite volume schemes for the compressible Euler and Navier–Stokes equations on unstructured adaptive grids, Ph.D. Thesis, University of Liege, Faculty of Applied Sciences, 1996.
[12] A. Dervieux, B. van Leer, J. Periaux, A. Rizzi (Eds.), Numerical Simulation of Compressible Euler Flows, Vieweg, Braunschweig, June 1989, GAMM Workshop, Proceedings of the GAMM Workshop on the Numerical Simulation of Compressible Euler flows, held at INRIA, Rocquencourt, France.
[13] A. Ferrante, H. Deconinck, Solution of the unsteady Euler equations using residual distribution and flux corrected transport, Project Report VKI PR 1997-08, Von Karman Institute for Fluid Dynamics, Belgium, June 1997.
[14] M. Hubbard, P. Roe, Compact high-resolution algorithms for time-dependent advection on unstructured grids, Internat. J. Numer. Methods Fluids 33 (5) (2000) 711–736.
[15] J. Maerz, Improving time accuracy for residual distribution schemes, Project Report 1996-17, Von Karman Institute for Fluid Dynamics, Belgium, Chausée do Waterloo 72, B-1640 Rhode Saint Genèse, Belgium, June 1996.
[16] M. Mezine, M. Ricchiuto, R. Abgrall, H. Deconinck, Monotone and stable residual distribution schemes on prismatic space–time elements for unsteady conservation laws, 33rd Computational Fluid Dynamics Course, Von Karman Institute for Fluid Dynamics, 2003.
[17] R.H. Ni, A multiple grid scheme for solving Euler equations, AIAA J. 20 (1) (1981).
[18] H. Paillère, Multidimensional upwind residual distribution schemes for the Euler and Navier–Stokes equations on unstructured grids, Ph.D. Thesis, Université Libre de Bruxelles, Von Karman Institute for Fluid Dynamics, June 1995.
[19] M. Ricchiuto, Construction and analysis of compact residual discretizations for conservation laws on unstructured meshes. Ph.D. Thesis, Université Libre de Bruxelles, Von Karman Institute for Fluid Dynamics, 2005.
[20] K. Sermeus, H. Deconinck, Drag prediction validation of a multi-dimensional upwind solver, CFD-based aircraft drag prediction and reduction, VKI Lecture Series 2003-02, Von Karman Institute for Fluid Dynamics, Chausée do Waterloo 72, B-1640 Rhode Saint Genèse, Belgium, 2003.